Eur Radiol (2012) 22:710–719
DOI 10.1007/s00330-011-2289-x

NUCLEAR MEDICINE

Prospective evaluation of ^{68}Ga-DOTA-NOC PET-CT in phaeochromocytoma and paraganglioma: preliminary results from a single centre study

Niraj Naswa · Punit Sharma · Aftab Hasan Nazar · Krishan Kant Agarwal · Rakesh Kumar · Ariachery C. Ammini · Arun Malhotra · Chandrasekhar Bal

Received: 5 July 2011 / Revised: 21 August 2011 / Accepted: 23 August 2011 / Published online: 5 October 2011

Abstract
Objective To evaluate the role of ^{68}Ga-labelled [1, 4, 7, 10-tetraazacyclododecane-1, 4, 7, 10-tetraacetic acid]-1-NaI^{3}-Octreotide (^{68}Ga-DOTA-NOC) whole body positron emission tomography-computed tomography (PET-CT) as a functional imaging approach for phaeochromocytoma and paraganglioma.
Methods Thirty-five unrelated patients (Median age-34.4 years; range: 15–71) were evaluated in this prospective study. PET-CT was performed after injection of 132–222 MBq of ^{68}Ga-DOTA-NOC. Images were evaluated by two experienced nuclear medicine physicians both qualitatively as well as quantitatively (standardised uptake value-SUVmax). In addition we compared the findings with ^{131}I Metaiodobenzylguanidine (MIBG) scintigraphy, which was available for 25 patients. Histopathology and/or conventional imaging with biochemical markers were taken as the reference standard.
Results 44 lesions were detected on ^{68}Ga-DOTA-NOC PET-CT imaging with an additional detection of 12 lesions not previously known, leading to a change in management of 6 patients. Sensitivity, specificity and accuracy were 100%, 85.7%, and 97.1% on a per patient basis and 100%, 85.7% and 98% on per lesion basis, respectively. ^{131}I MIBG scintigraphy was concordant with ^{68}Ga-DOTA-NOC PET-CT in 16 patients and false negative in 9 patients.
Conclusion ^{68}Ga-DOTA-NOC PET-CT is highly sensitive and specific for the detection of phaeochromoctyomas and paragangliomas. It seems better than ^{131}I MIBG scintigraphy for this purpose.
Key Points
- *^{68}Ga-DOTA-NOC PET-CT seems useful in patients with phaeochromocytoma and paraganglioma.*
- *This prospective single centre study showed that it has high diagnostic accuracy.*
- *^{68}Ga-DOTA-NOC PET-CT seems superior to ^{131}I-MIBG in these patients.*

Keywords Pheochromocytoma · Paraganglioma · ^{68}Ga-DOTA-NOC · PET-CT · MIBG

N. Naswa · P. Sharma · A. H. Nazar · K. K. Agarwal · R. Kumar · A. Malhotra · C. Bal (✉)
Department of Nuclear Medicine,
All India Institute of Medical Sciences,
Ansari Nagar, New Delhi 110029, India
e-mail: csbal@hotmail.com

A. C. Ammini
Department of Endocrinology and Metabolism,
All India Institute of Medical Sciences,
New Delhi, India

Introduction

Phaeochromocytomas are catecholamine producing tumours derived from the sympathetic nervous system [1, 2]. About 90% of these neoplasms occur as solitary benign tumours of the adrenal gland [3], and the rest can be localised in extra-adrenal sites [4]. About 10%–20% of the tumours are malignant [4]. In addition to sporadic forms, phaeochromocytomas are a feature of disorders with an autosomal dominant pattern of inheritance (e.g., multiple endocrine neoplasia type 2) in about one-fourth of unselected cases [4]. Phaeochromocytomas are the cause of hypertension in less than 1% of the hypertensive population, but they may be fatal if untreated or improperly treated. Thus,

precise localisation of phaeochromocytomas is critical to management [5, 6]. Paragangliomas, or glomus tumours, like phaeochromocytomas, arise from extra adrenal chromaffin tissue and frequently cause symptoms by over production of catecholamines [7]. About 9% of paragangliomas are familial [8]. Multicentricity of paragangliomas is present in about 10% of unselected series, but may be as high as 32% in familial cases [9]. Malignant behaviour occurs in about 10% of patients [9, 10].

The diagnosis of phaeochromocytoma/paragangliomas is established biochemically by measuring the level of urinary and plasma catecholamines and their metabolites (24-hour total metanephrine and/or catecholamine) [11]. However, imaging is important for the localisation of tumour and excluding possibility of multifocal lesions before surgery [12]. Computed tomography (CT) or magnetic resonance imaging (MRI) provide excellent morphologic details and have high sensitivity in the depiction of phaeochromocytoma, but they often fail to discriminate between phaeochromocytoma and other causes of adrenal gland enlargement [13] and occasional false positives can lead to unnecessary surgery [14]. Scintigraphy with ^{123}I metaiodobenzylguanidine (MIBG) is currently the functional imaging method of choice for the localisation of adrenal or extra-adrenal phaeochromocytomas and provides high sensitivity and specificity. However, it presents some disadvantages like-limited spatial resolution, difficult to detect tumours that are smaller than 1.5–2.0 cm in diameter, or when large tumours have extensive necrosis and/or haemorrhage, lack of tracer uptake in some tumours, interference with certain medications, all of which lead to false-negative results [15]. The targeted imaging of somatostatin receptors (SSTR 1–5) has given a new dimension to imaging of neuroendocrine tumours (NETs) [16]. Phaeochromocytomas and paragangliomas have also shown to express SSTR both on in vivo imaging and in vitro studies [17]. The single photon emission tomography (SPECT) agent ^{111}In-pentetreotide has been shown to be superior to MIBG in patients with malignant, metastatic and extra-adrenal lesions. However, the overall sensitivity of this method is less than 30% [18]. ^{68}Ga-labelled [1, 4, 7, 10–tetraazacyclododecane-1, 4, 7, 10-tetraacetic acid]-1-NaI^{3}-Octreotide (^{68}Ga-DOTA-NOC) is a positron emission tomography (PET) tracer for somatostatin receptor scintigraphy (SRS), which provides the advantages of better resolution and quantification, of PET technology. ^{68}Ga-DOTA-NOC PET-CT has already been proven to be of great value in NET. However, there is limited literature regarding its use in phaeochromocytoma and paraganglioma. Therefore, the purpose of the present study was to evaluate the role of ^{68}Ga-DOTA-NOC PET-CT in patients known or suspected to have either phaeochromocytoma or paraganglioma.

Materials and methods

From Oct 2006 to June 2010, 35 consecutive unrelated patients with known or suspected Phaeochromocytoma or paraganglioma were referred to our institution for ^{68}Ga-DOTA-NOC PET-CT and were included in this prospective study. The study was conducted in accordance with the institute's ethics protocol and written informed consent was obtained from all patients.

^{68}Ga-DOTA-NOC PET-CT acquisition

^{68}Ga-DOTA-NOC synthesis was carried as previously detailed by Zhernosekov et al [19] and imaging was performed on a dedicated PET-CT system (Biograph 2, Siemens Medical Solutions, Erlangen, Germany). Fasting was not mandatory. A dose of 132–222 MBq (4–6 mCi) of ^{68}Ga-DOTA-NOC was injected intravenously. After a 45–60 min uptake period the patients were taken for PET-CT. Oral contrast agent was used. No intravenous contrast agent was used. In the PET-CT system, CT acquisition was performed on spiral dual slice CT with a slice thickness of 4 mm and a pitch of 1. Image was acquired using a matrix of 512×512 pixels and pixel size of 1 mm. After CT acquisition, the table was moved towards the field of view of PET and PET acquisition of the same axial range was started with the patient in the same position. The PET components of the PET-CT are based on a full-ring lutetium oxyorthosilicate (LSO) PET system. 3D PET acquisition was done from base of skull (including pituitary fossa) to mid thighs. PET data were acquired using matrix of 128×128 pixels with a slice thickness of 1.5 mm. CT based attenuation correction of the emission images was employed. PET images were reconstructed by iterative method ordered subset expectation maximisation (OSEM; 2 iterations and 8 subsets). After completion of PET acquisition, the reconstructed attenuation corrected PET images, CT images and fused images of matching pairs of PET and CT images were available for review in axial, coronal and sagittal planes, as well as in maximum intensity projections (MIP), three dimensional mode.

^{131}I MIBG Scintigraphy

None of the patients received any drugs that would interfere with MIBG uptake, such as tricyclic antidepressants, or sympathomimetic amines. We could not use ^{123}I MIBG as it is not available at our centre. Following the intravenous injection of a mean dose of 37±12 MBq of ^{131}I- MIBG (GE Healthcare, Braunschweig, Germany), planar scintigraphic images was obtained with a large field of view dual head gamma camera (Symbia E, Siemens medical solutions, Illinois, USA) and a high energy collimator. Twenty-four

and 48 h after injection, whole-body images in the ventral and dorsal planes, as well as target images of the abdomen and thorax, were acquired. Single photon emission computed tomography (SPECT) of the thorax and abdomen was performed 24 h after injection by using a double head camera and the following parameters: a 128×128 matrix, 120 projections in 3° angle increments, and an acquisition time of 40 s per projection. Image reconstruction was performed by using filtered back projection, with no prefiltering, reconstruction with a ramp filter, and post processing with a low-pass filter.

Interpretation of ^{68}Ga-DOTA-NOC PET-CT and ^{131}I MIBG Scintigraphy

^{68}Ga-DOTA-NOC PET-CT and ^{131}I MIBG scintigraphy were evaluated by two experienced Nuclear medicine physicians. Both the reviewers were in total agreement for 34/35 cases on ^{68}Ga-DOTA-NOC PET-CT and 23/25 cases on ^{131}I MIBG scintigraphy. For the remaining cases a consensus diagnosis was reached. They were blinded to findings of the structural imaging and clinical findings. PET images were evaluated both qualitatively and semi-quantitatively. Positive findings on ^{68}Ga-DOTA-NOC PET were localised to anatomical images from the non enhanced CT. Any increased accumulation of ^{68}Ga-DOTA-NOC in the adrenal glands or extra-adrenal regions was considered abnormal, with corresponding lesion on CT was considered abnormal. The size and maximum standardised uptake value (SUVmax) of the lesions were calculated.

Planar and SEPCT MIBG images, which were obtained 24 and 48 h after injection, were included for assessment of MIBG scintigraphy. Any focal accumulation of MIBG in the adrenal glands or extra-adrenal regions that exceeded the normal regional tracer uptake was considered abnormal. MIBG images were evaluated in separate sessions to avoid bias.

Reference standard

Histopathology (HPE) results were available for 13 patients that underwent surgery. In the remaining 22 patients the results of ^{68}Ga-DOTA-NOC PET-CT were compared with conventional imaging and/or follow up imaging in combination with biochemical markers and MIBG scintigraphy, as tumour biopsy is contraindicated in these groups of neoplasms.

Statistical analysis

Continuous variables were expressed as the median and range. Categorical data were expressed as number and percentage. Sensitivity, specificity, accuracy, positive (PPV) and negative predictive value (NPV) of ^{68}Ga-DOTA-NOC PET-CT were calculated on per patient and per lesion basis. Mann Whitney test with two tailed probability was used to compare groups. Spearman's rank correlation coefficient was used to correlate any relation between tumour size and the standardised uptake value (SUVmax) on PET-CT. McNemar test was used to compare the diagnostic accuracy of ^{68}Ga-DOTA-NOC PET-CT with MIBG scintigraphy. All the data analyses were performed using the statistical software packages SPSS 11.5(SPSS Inc., Chicago, Illinois, USA).

Results

Patient characteristics

Patient characteristics including ages, sex, and indication of PET-CT are outlined in Table 1.

Results of ^{68}Ga-DOTA-NOC PET-CT

Patient-wise analysis

^{68}Ga-DOTA-NOC PET-CT imaging was very useful in the localisation and detection of these tumours (Table 2). Of the 35 patients that underwent the study, ^{68}Ga-DOTA-NOC PET-CT was positive in 29 patients and negative in 6 patients. There was one false positive result as the adrenal tumour defined as a phaeochromocytoma turned out to be a benign adrenal adenoma on HPE. Of the 6 patients that were negative on ^{68}Ga-DOTA-NOC PET-CT, an alternative diagnosis was suggested later on follow-up. Thus the overall sensitivity, specificity and accuracy on a per patient basis were 100% (95% CI-87.5–100), 85.7% (95% CI-42.2–97.6), and 97.1%, with a PPV of 96.5% (95% CI-82.1–99.4) and NPV of 100% (95% CI-54–100).

Table 1 Patient characteristics

Variable	Values	%
Age (years)		
Median	34.4	–
Range	15–71	–
Sex		
Male	22	62.8
Female	13	37.2
Weight (Kg)		
Median	62	–
Range	46–74	–
Indication for PET-CT		
Known	14	40
Suspected	21	60

Table 2 A patient wise summary of ^{68}Ga-DOTANOC PET-CT findings

No	Age (years)	Sex	Clinical Presentation	Indication	68Ga-DOTANOC PET-CT	Findings	Largest Size (cm)	SUVmax	Other Functional Imaging	Detection of extra foci	Final Diagnosis
1	40	F	HTN	Suspected	Pos	Lt Adr	1.4	23.1	FDG, MIBG, FDOPA	No	Pheo
2	46	F	Headache	Suspected	Pos	Lt Adr	11	6.4	ND	No	Pheo
3	30	F	HTN	Known	Pos	Rt Adr	1.5	5	MIBG	No	Adenoma
4	37	F	Tinnitus, Facial palsy	Known	Pos	Bl CBT, Glo.tym Aortic body, Abd PGL	4.9	61	FDG	Yes	Multifocal PGL
5	24	M	HTN, Headache	Suspected	Pos	Rt Adr	4	5	FDG, MIBG	No	Pheo
6	30	F	HTN	Suspected	Neg	–	–	–	MIBG	–	RAS
7	35	M	HTN, neck mass	Known	Pos	Glo.jug	5.5	3	NA	No	Glo.jug
8	37	F	HTN	Suspected	Pos	Bl Adr, Thyroid	4.2	74.2	MIBG	Yes	MEN 2B
9	56	M	HTN	Suspected	Pos	Rt Adr	10	259	FDG	No	Pheo
10	47	F	Abd pain, HTN	Suspected	Pos	Abd PGL	7	78.3	MIBG	No	Abd PGL
11	48	M	HTN, Palpitations	Suspected	Neg	–	–	–	MIBG	–	EH
12	16	M	HTN retinopathy	Suspected	Pos	Rt Adr	3.7	14	MIBG	No	Pheo
13	18	M	HTN	Known	Pos	Mediastinum, Bladder	4	13.4	MIBG	No	Multifocal PGL
14	35	F	HTN	Known	Pos	Rt Adr	8	15.6	ND	No	Pheo
15	26	M	Headache, HTN	Suspected	Neg	–	–	–	MIBG	–	Renal
16	45	M	Neck mass, Tinnitus	Known	Pos	BL CBT, Bl Glo.jug, Bone	8.5	65	ND	Yes	Malignant PGL
17	19	M	Headache ,HTN	Suspected	Pos	Abd mass	3	15.6	MIBG	No	Abd PGL
18	28	F	BL neck mass	Known	Pos	BL CBT	1.8	23.8	MIBG	No	PGL
19	40	M	Neck mass	Known	Pos	Lt CBT	3.5	15.5	MIBG	No	PGL
20	15	M	RP mass	Suspected	Pos	RP mass	4.2	7	FDG	No	PGL
21	35	F	HTN	Known	Pos	Lt Glo.jug	4.2	5.1	MIBG	No	PGL
22	20	M	HTN	Suspected	Pos	Rt Adr	3.3	6.9	MIBG, FDOPA	No	Pheo
23	16	M	HTN	Suspected	Pos	Rt Adr	2.9	8.9	MIBG	No	Pheo
24	30	M	HTN	Suspected	Neg	–	–	–	MIBG	–	Renal
25	50	F	HTN	Suspected	Pos	Lt Adr	2.9	7.1	MIBG, FDOPA	No	Pheo
26	20	F	Facial palsy, Hearing loss	Known	Pos	Rt Glo.jug	4.6	4	MIBG	No	PGL
27	37	M	HTN	Known	Pos	BL Adr	4.1	13.6	MIBG, FDOPA	Yes	BL Pheo
28	33	M	BL Neck mass	Known	Pos	BL CBT, Rt Glo.jug	2.9	8.7	ND	Yes	Multifocal PGL
29	37	M	HTN	Suspected	Neg	–	–	–	MIBG	–	EH
30	19	M	HTN	Known	Pos	RP mass	2.5	12.2	FDG, MIBG	No	PGL
31	39	M	Asymptomatic	Suspected	Pos	Abd mass	1.5	14	FDG, MIBG	No	PGL
32	45	M	Neck mass	Suspected	Pos	Parapharyngeal mass, Lung	4	17	FDG	Yes	Malignant PGL
33	43	F	HTN	Suspected	Neg	–	–	–	MIBG	–	EH
34	40	M	HTN	Known	Pos	Rt Adr	4	40	FDG, MIBG	No	Pheo
35	71	M	HTN	Suspected	Pos	Rt Adr	4.7	8	FDG	No	Pheo

HTN Hypertension; *Adr* Adrenal; *FDOPA* F18 Fluoro-dihydroxyphenylalanine; *FDG* F18 Flurodeoxyglucose; *MIBG* I131 Metaiodobenzylguanidine; *Pheo* Pheochromocytoma; *PGL* paraganglioma; *RAS* renal artery stenosis; *EH* Essential hypertension; *CBT* carotid body tumor; *Glo.jug* Glomus jugulare; *Glo.tym* Glomus tympanicum

Table 3 Comparative diagnostic accuracy of ^{68}Ga-DOTANOC PET-CT and ^{131}I MIBG scintigraphy (lesion wise)

Parameter	MIBG	PET-CT
Sensitivity	64% (42.5–81.9)	100% (86.1–100)
Specificity	85.7% (42.2–97.6)	85.7% (42.2–97.6)
PPV	94.1% (71.2–99)	96.1% (80.3–99.3)
NPV	40% (16.4–67.6)	100% (55–100)
Accuracy	68.7%	96.8%

PPV positive predictive value; *NPV* negative predictive value

Lesion-by-lesion analysis

A total of 44 lesions were seen on ^{68}Ga-DOTA-NOC PET-CT imaging with one false-positive result (adenoma). The overall sensitivity, specificity and accuracy on a per lesion basis were: 100% (95% CI-91.7–100), 85.7% (95% CI-42.2–97.6), and 98%, with a PPV of 97.7% (95% CI-87.9–99.6) and NPV of 100% (95% CI-54–100). There was detection of 12 extra lesions when compared with their preliminary findings based on conventional imaging.

Correlation of lesion size with SUVmax

The mean tumour size was 3.7 cm±2.31(range: 1–11 cm) while the mean SUVmax was 25.3±23.9 (range: 1.4–89.1). We evaluated the relationship between lesion size and their respective SUVmax to see whether tumour size correlated with somatostatin expression. No significant relationship between size of tumour and SUVmax was seen (P=0.755) [Fig. 1].

Results of semi-quantitative analysis

A total of 15 adrenal and 29 extra-adrenal tumours were detected on ^{68}Ga-DOTA-NOC PET-CT imaging. The median SUVmax value of adrenal tumours was 10.9 (range-5–74.2). Although the median SUVmax of paragangliomas was higher (SUVmax −17; range-1.4–89.1) than adrenal lesions, there was no overall significant difference in the level of tracer uptake (P=0.197). Of the paragangliomas, 17 were head and neck paragangliomas while the rest were detected in mediastinum, abdomen and urinary bladder. There was no significant difference in SUVmax of head and neck vs. other paragangliomas (p=0.822).

Comparison of ^{68}Ga-DOTA-NOC PET-CT with ^{131}I-MIBG

Both ^{68}Ga-DOTA-NOC PET-CT and ^{131}I-MIBG were available in 25 patients. The comparison of results of ^{68}Ga-DOTA-NOC PET-CT and ^{131}I-MIBG is given in Table 3. ^{68}Ga-DOTA-NOC PET-CT was superior to ^{131}I-MIBG (P=0.003). Only one of the 26 lesions that were considered to be positive on ^{68}Ga-DOTA-NOC PET-CT imaging turned to be false positive (adenoma on HPE), while the rest 25 lesions were true positive. On the other hand, ^{131}I-MIBG scintigraphy showed 16 true positive lesions (Figs. 2 and 3). No MIBG uptake was seen in 9 lesions which were positive on ^{68}Ga-DOTA-NOC PET-CT (Fig. 4). The patient with adenoma was false positive on ^{131}I-MIBG imaging as well. Most of the lesions that were negative on ^{131}I-MIBG scintigraphy were extra-adrenal (paragangliomas) (Table 4).

Discussion

Diagnosing and locating phaeochromocytomas can be a challenging experience for clinicians, because these tumours can mimic a variety of other diseases and the primary tumours can occur in varying locations. MIBG (I123/I131) scintigraphy has been considered the gold standard; however it suffers from many drawbacks. Even in our series where ^{131}I MIBG results were available with 25 patients, it was falsely negative in 9 patients with most of them having extra-adrenal (paragangliomas) lesions.

Thus far, there has been little experience with PET imaging of phaeochromocytomas. Previously, ^{18}F-Fluorodeoxyglucose (FDG) PET has not been widely used in oncoendocrinology because of a lack of specificity [20]. Two different studies by Taïeb et al. and Shuklin et al, opined that most phaeochromocytomas accumulate FDG especially the malignant variety and can be more useful in defining the distribution of those phaeochromocytomas that fail to concentrate MIBG. Another useful remark by this study was to refrain from concluding that absence of FDG uptake excludes phaeochromocytoma [21, 22]. Other PET based radionuclides like ^{11}C Hydroxyephedrine and ^{18}F-Flurorodihydroxyphenylalanine (FDOPA) have also been evaluated in such tumours with both providing a high level of accuracy in these group of tumours [23, 24].

In our study, SRS with PET tracer ^{68}Ga-DOTA-NOC PET-CT was evaluated as a diagnostic tool and implicated as a potential new strategy for imaging of phaeochromocytomas and paragangliomas. It has been previously been evaluated in several other NETs [25, 26] with very good results. To our knowledge though, systematic studies using ^{68}Ga-DOTA-NOC in the detection of phaeochromocytomas and paragangliomas has not been described in the literature till date. Only one small series by Win et al, have compared the PET tracer ^{68}Ga-DOTA-TATE with ^{123}I-MIBG in five patients with phaeochromocytoma [27]. In that series ^{68}Ga-DOTA-TATE PET showed more lesions, with higher uptake and better resolution, compared with

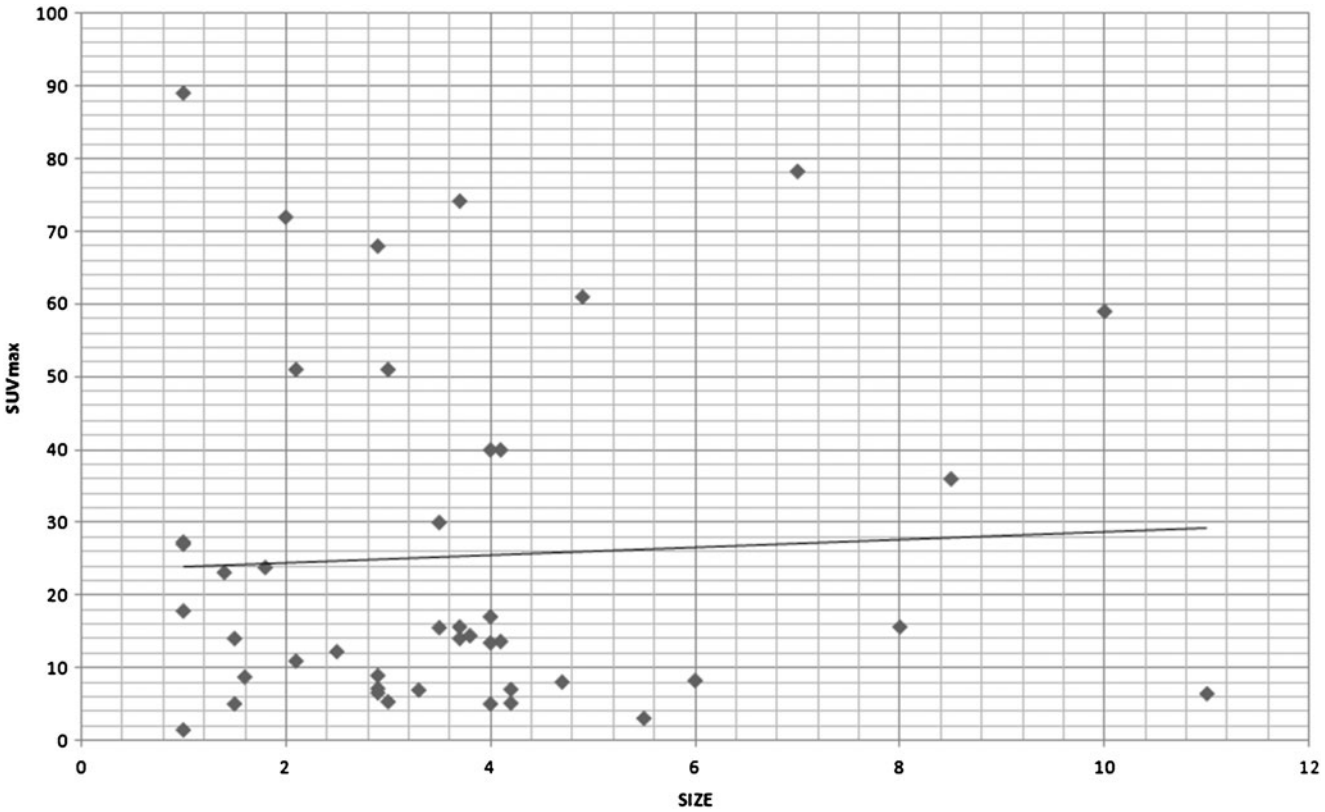

Fig. 1 Dot and line diagram showing relation between SUVmax of tumour and tumour size. No significant correlation was found (P=0.755)

^{123}I-MIBG. However, that study differs from the present study in many important aspects: very small sample size, use of ^{68}Ga-DOTA-TATE which has affinity for limited spectrum of SSTRs compared with ^{68}Ga-DOTA-NOC, use of PET and not PET-CT and use of ^{123}I-MIBG as compared with ^{131}I-MIBG used in present study. In our series of 35 patients, ^{68}Ga-DOTA-NOC PET-CT had diagnostic accuracy of 97.1% on per patient and 98% on lesions wise analysis. ^{68}Ga-DOTA-NOC PET-CT was negative in 6 patients. Although they had higher than normal levels of catecholamines and clinical symptoms of hypertension compatible with a diagnosis of phaeochromocytoma, one might argue as to the result of ^{68}Ga-DOTA-NOC PET-CT be considered as false-negative in these 6 patients. However, these patients also had normal conventional imaging results (except 1 patient who had an adrenal lesion with negative ^{68}Ga-DOTA-NOC uptake) and even negative MIBG studies as well and were offered an alternative diagnosis on further follow-up (essential hypertension in 4, and renal artery stenosis in 2 patients). These situations are not uncommon in clinical practice. A large survey revealed that 4.2% of incidentalomas were phaeochromocytomas, but only 43% of these patients were hypertensive, despite urinary catecholamine elevations in 86% [28]. Results of ^{68}Ga-DOTA-NOC PET-CT were therefore considered as true negative in these patients and stress the importance of this imaging technique in ruling out such tumours apart from diagnosing and localisation at the same time.

^{68}Ga-DOTA-NOC PET-CT also led to a change in management in 6 patients with 2 of them spared unnecessary surgery. There was additional detection of 12 lesions over and above the 32 lesions defined on baseline Conventional imaging (CI). In one patient there was detection of multiple vertebral metastases in a patient who had multiple head and neck paragangliomas. In another patient who presented with severe hypertension and bilateral phaeochromocytomas, an additional focus was detected in the right lobe of thyroid gland which revealed features of medullary carcinoma thyroid on histology. A diagnosis of MEN-IIa was made in this patient that has a different approach for follow-up. In addition, the demonstration of SSTR expression by such neoplasms may give an opportunity to treat them using peptide based radioreceptor therapy (PRRT). There was however no significant relationship between the degree of tracer uptake (SUVmax) and lesion size and or between adrenal and extra-adrenal lesions.

From in vitro and in vivo studies, it has been established that somatostatin receptor subtypes 3 and 4 are expressed in phaeochromocytoma, including extra-adrenal and metastatic disease [29]. Usually the expression of SSTR receptors is increased in malignant phaeochromocytomas

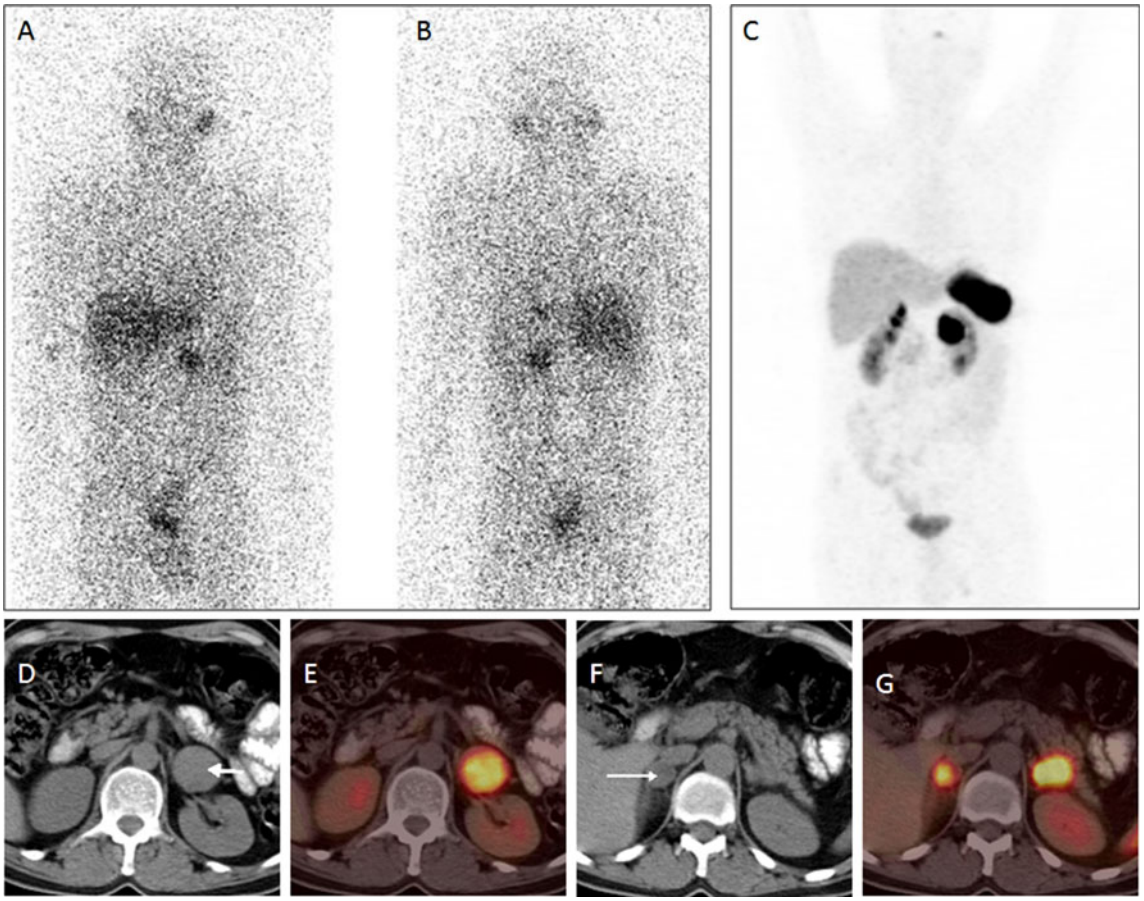

Fig. 2 A 37 year old male patient with hypertension and elevated plasma and urinary catecholamines. ^{131}I MIBG images (**A**, **B**) show increased uptake in left adrenal region. ^{68}Ga DOTA-NOC maximum intensity projection (MIP) image (**C**) show increase tracer uptake in bilateral adrenal regions. CT (**D**, **F**) and PET-CT (**E**, **G**) images show bilateral adrenal masses (left > right) with increased tracer uptake. A diagnosis of bilateral adrenal phaeochromoctyoma was made and confirmed with histopathology. In this patient right adrenal lesion missed on ^{131}I MIBG was seen on ^{68}Ga DOTA-NOC PET-CT

and paragangliomas [30]. Previous studies with ^{111}In-Octerotide have shown higher sensitivity for detecting metastatic phaeochromocytoma than for detecting benign phaeochromocytoma [31]. Apart from the issue of limited resolution, this might have also been because of the fact that ^{111}In-Octreotide has predominant affinity towards SSTR 2. In our study ^{68}Ga-DOTA-NOC PET-CT showed high sensitivity for both phaeochromocytoma and paragangliomas. This is partly because of wide spectrum of affinity of ^{68}Ga-DOTA-NOC for SSTR subtypes. Uptake of ^{131}I MIBG is on the other hand dependent on the expression of vesicular monoamine transporters (VMAT 1,2). Expression of VMAT is high in benign phaeochromocytoma, but is reduced in malignant phaeochromocytoma and paragangliomas. Indeed, Kolby et al have shown that even in malignant phaeochromocytoma/paragangliomas high MIBG uptake is seen in tumours with high VMAT 1,2 expression as compared with no MIBG uptake in tumours with low VMAT 1,2 expression [32]. In our study also ^{131}I MIBG scintigraphy was mainly false negative in paragangliomas (n=5). However, as the expression profile for VMAT was not available for this patient population we were unable to correlate it with MIBG uptake. This in vivo demonstration of VMAT (with MIBG) and SSTR (with ^{68}Ga-DOTA-NOC) has important implications regarding therapy of these tumours, especially when inoperable or malignant, for selecting appropriate radionuclide therapy.

Another important factor to be taken into account is the germline mutations in genes encoding one of the subunits of the mitochondrial complex II succinate dehydrogenase (SDH) enzyme gene, a component of the tricarboxylic acid cycle [33]. Paragangliomas and more rarely phaeochromocytomas can occur as a part of familial paraganglioma syndromes (PGL 1–4) secondary to SDH mutations. Such tumours have the highest risk of malignancy and death [34]. Thus, SDH status appears to be critical parameter determining the prognosis as well as selecting the best functional imaging agent for phaeochromocytomas and paragangliomas. Given their extraadrenal location and malignant nature

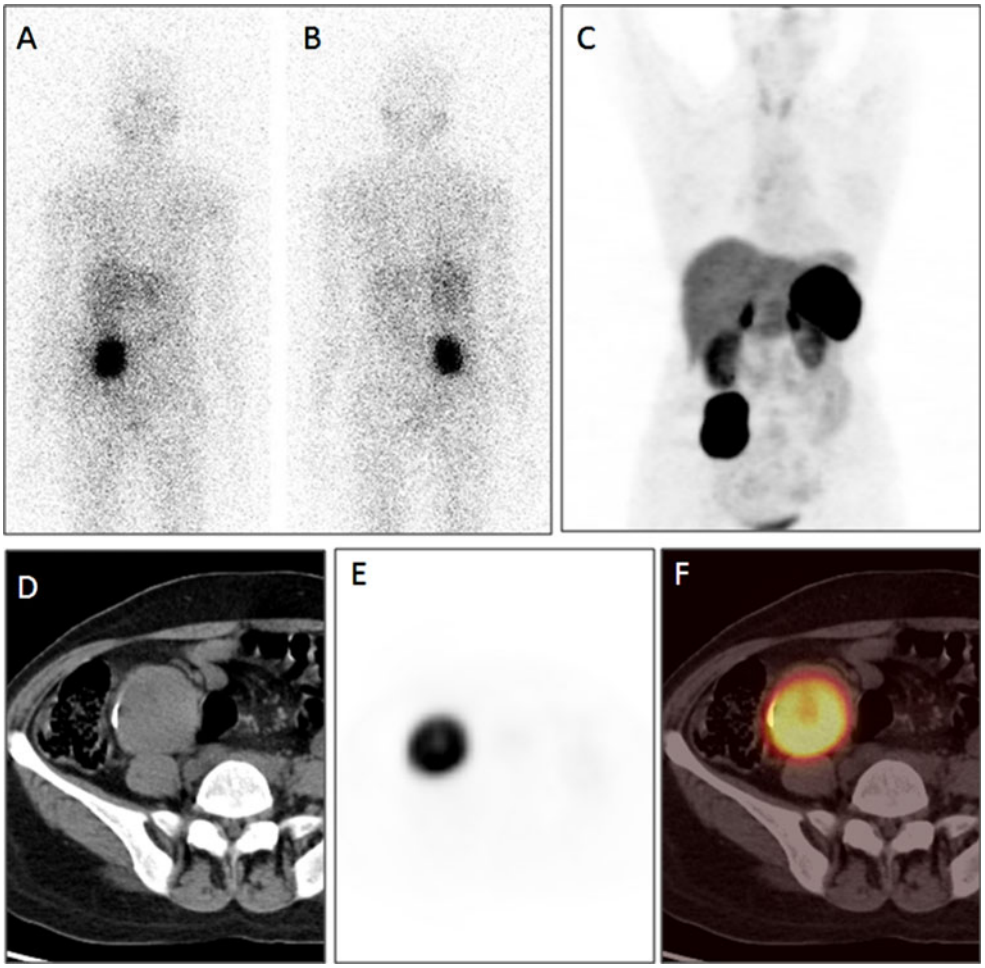

Fig. 3 A 47-year-old female patient presenting with abdominal pain, hypertension and elevated urinary catecholamines. ^{131}I MIBG images (**A**, **B**) show increased uptake in right side of abdomen. ^{68}Ga DOTA-NOC maximum intensity projection (MIP) image (**C**) show increase tracer uptake in same region. CT (**D**), PET (**E**) and PET-CT (**F**) images show an abdominal mass with calcification, and intense uptake of ^{68}Ga DOTA-NOC (SUVmax-78.3). A diagnosis of paraganglioma was made and confirmed with histopathology

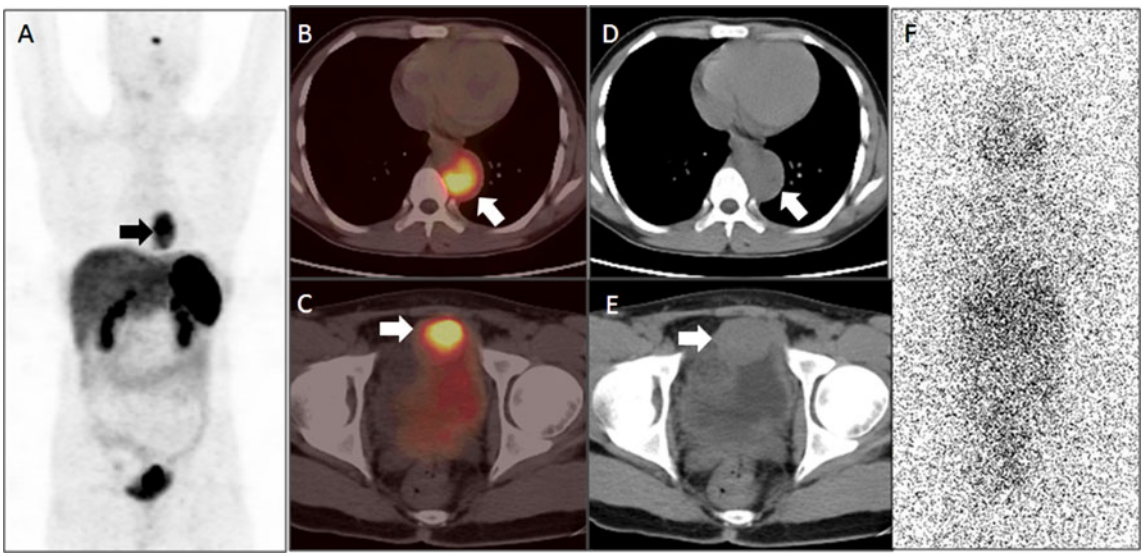

Fig. 4 An 18-year-old male patient presenting with hypertension. On further evaluation plasma and urinary catecholamines were raised and he underwent ^{68}Ga DOTA-NOC PET-CT. Maximum intensity projection (MIP) image (**A**) showed one focus of tracer uptake in mediastinum (*arrow*) and other suspicious focus adjacent to bladder. PET-CT and CT images of mediastinum (**B**, **D**) showed ^{68}Ga DOTA-NOC concentrating posterior mediastinal mass (*arrow*). Interestingly, a bladder mass with ^{68}Ga DOTA-NOC uptake (*arrow*) was seen in pelvic PET-CT and CT image (**C**, **E**). ^{131}I MIBG scintigraphy (**F**) in this patient was essentially normal. The patient underwent surgery and the diagnosis was confirmed on histopathology

Table 4 Tumor size, tumor type and results of ^{131}I MIBG scintigraphy as compared to ^{68}Ga-DOTA-NOC PET-CT

No.	Tumor size (cm)	Tumor type (Final Diagnosis)	^{131}I MIBG	^{68}Ga-DOTA-NOC PET-CT
1	1.2×1.4	Pheochromocytoma	TP	TP
2	1×1.5	Adenoma	FP	FP
3	3×4	Pheochromocytoma	TP	TP
4	–	None; Renal Artery Stenosis	TN	TN
5	3.7×4.2 (Rt Adr)	Pheochromocytoma (MEN-IIb)	TP	TP
	2.7×3 (Lt Adr)		TP	TP
6	5.4×7	Paraganglioma (Abdomen)	TP	TP
7	–	None; Essential HTN	TN	TN
8	3×3.7	Pheochromocytoma	FN	TP
9	2×3	Paraganglioma (Post Mediastinum, Urinary Bladder)	FN	TP
	3×4		FN	TP
10	–	None; Reno-vascular HTN	TN	TN
11	3×3.7	Paraganglioma (Abdomen)	FN	TP
12	2.4×3.8	Head and Neck Paraganglioma	TP	TP
13	2.6×3.5	Head and Neck Paraganglioma	TP	TP
14	3.2×4.2	Head and Neck Paraganglioma	FN	TP
15	2.2×3.3	Pheochromocytoma	TP	TP
16	2.3×2.9	Pheochromocytoma	TP	TP
17	–	None; Reno-vascular HTN	TN	TN
18	2.7×2.9	Pheochromocytoma	TN	TN
19	4.4×6	Head and Neck Paraganglioma	FN	TP
20	2×2.1 (Rt Adr)	Pheochromocytoma	FN	TP
	3.3×4.1 (Lt Adr)		TP	TP
21	–	None; Essential HTN	TN	TN
22	2.2×2.5	Paraganglioma (Retroperitoneal)	TP	TP
23	1×1.5	Paraganglioma (Abdomen)	TP	TP
24	–	None; Essential HTN	TN	TN
25	2.3×4	Pheochromocytoma	TP	TP

HTN Hypertension; *Adr* Adrenal; *TP* True positive; *TN* True Negative; *FP* False Positive; *FN* False Negative

it appears that ^{68}Ga-DOTA-NOC PET-CT will be more useful than ^{131}I-MIBG in patients with SDH mutations. In turn ^{131}I-MIBG may be better suited for non SDH mutation associated tumours. Since, SDH status was not available for our patient population we are unable to make any such analysis in the present study.

The study is not without limitations. Firstly, the number of patients was limited due the rarity of disease. Secondly, not all lesions could be verified histologically. Moreover, the profile of SSTR expression by the tumours and the SDH status were not available in the present study. If present, this would have given important information regarding tumour biology. Especially, the lack of knowledge regarding the SDH status, as it is pivotal to understanding the results of functional imaging of these tumours. This was a major limitation of present study. Thirdly, there were 44 masses in 35 patients but no clustering analysis was done. Fourthly, we used ^{131}I MIBG and not ^{123}I MIBG, which is a superior tracer for phaeochromoctyoma with better image quality. This is because of non-availability of ^{123}I MIBG in our country. Also, we did not compare MIBG SPECT-CT with PET-CT. A larger prospective study with use of ^{123}I MIBG SPECT-CT for comparison will further validate this study.

Conclusion

In conclusion, results of present study show that ^{68}Ga-DOTA-NOC PET-CT is an imaging technique that provides high sensitivity and specificity in the detection of phaeochromocytomas and paragangliomas and is superior to ^{131}I MIBG scintigraphy. ^{68}Ga-DOTA-NOC PET-CT has the potential to become the functional imaging method of choice, after the results reported herein are confirmed in a larger patient population.

References

1. Gifford RW Jr, Manger WM, Bravo EL (1994) Pheochromocytoma. Endocrinol Metab Clin North Am 23:387–404
2. Werbel SS, Ober KP (1995) Pheochromocytoma: update on diagnosis, localization, and management. Med Clin North Am 79:131–153
3. Manger WM, Gifford RW (1995) Pheochromocytoma: a clinical overview. In: Laragh JH, Brenner BM (eds) Hypertension: pathophysiology, diagnosis and management. Raven, New York, pp 225–244
4. Neumann HPH, Berger DP, Sigmund G et al (1993) Pheochromocytomas, multiple endocrine neoplasia type 2, and von Hippel-Lindau disease. N Engl J Med 329:1531–1538
5. Moreira SG Jr, Pow-Sang JM (2002) Evaluation and management of adrenal masses. Cancer Control 9:326–334
6. Bravo EL (1994) Evolving concepts in the pathophysiology, diagnosis and treatment of pheochromocytoma. Endocr Rev 15:356–368
7. CapellaC RivaC, Cornaggia M et al (1988) Histopathology, cytology and cytochemistry of pheochromocytomas and paragangliomas including chemodectomas. Path Res Pract 183:176–187
8. Grufferman S, Gillman MW, Pasternak LR et al (1980) Familial carotid body tumors: case report and epidemiologic review. Cancer 46:2116–2122
9. Kliewer KE, Wen DR, Cancilla PA et al (1989) Paragangliomas: assessment of prognosis by histologic, immunohistochemical, and ultrastructural techniques. Hum Pathol 20:29–39
10. Lack EE, Cubilla AL, Woodruff JM (1979) Paragangliomas of the head and neck region. A pathologic study of tumors from 71 patients. Hum Pathol 10:191–218
11. Kudva YC, Sawka AM, Young WF Jr (2003) Clinical review 164: the laboratory diagnosis of adrenal pheochromocytoma—the Mayo Clinic experience. J Clin Endocrinol Metab 88:4533–4539
12. Neumann HPH, Bender BU, Reincke M et al (1999) Adrenal sparing surgery for pheochromocytoma. Br J Surg 84:94–97
13. Quint LE, Glazer GM, Francis IR et al (1987) Pheochromocytoma and paraganglioma: comparison of MRI imaging with CT and ^{131}I MIBG scintigraphy. Radiology 165:89–93
14. Connor CS, Hermreck AS, Thomas JH (1988) Pitfalls in the diagnosis of pheochromocytoma. Am Surg 54:634–636
15. Khafagi FA, Shapiro B, Fig LM et al (1989) Labetalol reduces ^{131}I MIBG uptake by pheochromocytoma and normal tissues. J Nucl Med 30:481–489
16. Patel YC (1999) Somatostatin and its receptor family. Front Neuroendocrinol 20:157–198
17. Jochen M, Nicole U, Stefan S et al (2003) Somatostatin Receptor Subtypes in Human Pheochromocytoma: Subcellular Expression Pattern and Functional Relevance for Octreotide Scintigraphy. J Clin Endocrinol Metab 88:5150–5157
18. Van der Harst E, De Herder WW, Bruining HA et al (2000) 123[I] Metaiodobenzylguanidine and 111[In] octreotide uptake in benign and malignant pheochromocytomas. J Clin Endocrinol Metab 86:685–693
19. Zhernosekov KP, Filosofov DV, Baum RP et al (2007) Processing of Generator-Produced ^{68}Ga for Medical Application. J Nucl Med 48:1741–1748
20. Eriksson B, Orlefors H, Oberg K et al (2005) Developments in PET for the detection of endocrine tumours. Best Pract Res Clin Endocrinol Metab 19:311–324
21. Taïeb D, Sebag F, Barlier A et al (2009) ^{18}F-FDG Avidity of Pheochromocytomas and Paragangliomas: A New Molecular Imaging Signature? J Nucl Med 50:711–717
22. Shuklin BL, Thompson NW, Shapiro B et al (1999) Pheochromocytomas: Imaging with 2-[Fluorine-18] fluoro-2-deoxy-D-glucose PET. Radiology 212:35–41
23. Trampal C, Engler H, Juhlin C et al (2004) Pheochromocytomas: Detection with ^{11}C Hydroxyephedrine PET. Radiology 230:423–428
24. Hoegerle S, Nitzsche E, Altehoefer C et al (2002) Pheochromocytomas: Detection with ^{18}F DOPA Whole-Body PET—Initial Results. Radiology 222:507–512
25. Ambrosini V, Campana D, Bodei L et al (2010) ^{68}Ga-DOTA-NOC PET/CT Clinical Impact in Patients with Neuroendocrine Tumors. J Nucl Med 51:669–673
26. Maecke HR, Hofmann M, Haberkorn U (2005) ^{68}Ga-Labeled Peptides in Tumor Imaging. J Nucl Med 46:172S–178S
27. Win Z, Al-Nahhas A, Towey D et al (2007) 68Ga-DOTATATE PET in neuroectodermal tumours: first experience. Nucl Med Commun 28:359–363
28. Mantero F, Massimo T, Arnoldi G et al (2000) A survey on adrenal incidentaloma in Italy. J Clin Endocrinol Metab 85:637–644
29. Ueberberg B, Tourne H, Redman A et al (2005) Differential expression of the human somatostatin receptor subtypes sst1 to sst5 in various adrenal tumors and normal adrenal gland. Horm Metab Res 37:722–728
30. van der Harst HE, de Herder WW, Bruining HA et al (2001) (123) I metaiodobenzylguanidine and (111)In octreotide uptake in benign and malignant pheochromocytomas. J Clin Endocrinol Metab 86:685–693
31. Kaltsas G, Korbonits M, Heintz E et al (2001) Comparison of somatostatin analog and meta-iodobenzylguanidine radionuclides in the diagnosis and localization of advanced neuroendocrine tumors. J Clin Endocrinol Metab 86:895–902
32. Kölby L, Bernhardt P, Johanson V et al (2006) Can quantification of VMAT and SSTR expression be helpful for planning radionuclide therapy of malignant pheochromocytomas? Ann N Y Acad Sci 1073:491–497
33. Timmers H, Gimenez-Roqueplo AP, Mannelli M, Pacak K (2009) Clinical aspects of SDHx-related pheochromocytoma and paraganglioma. Endocr Relat Cancer 16:391–400
34. Burnichon N, Rohmer V, Amar L et al (2009) The succinate dehydrogenase genetic testing in a large prospective series of patients with paragangliomas. J Clin Endocrinol Metab 94:2817–2827